Digest Journal of Nanomaterials and Biostructures Vol. 11, No. 2, April - June 2016, p. 477 - 488

SYNTHESIS, STUDY OF ELECTRICAL, THERMAL BEHAVIOR OF POLYPYRROLE, POLYANILINE AND POLYANILINE -POLYSTYRENE SULPHONIC ACID COMPOSITE

G. MURTAZA[a,c*], I. AHMAD[a], A. HAKEEM[b], P. MAO[c], X. GUOHUA[c]
[a]*Department of Physics, Bahauddin Zakariya University, Multan 60800 Pakistan*
[b]*Department of Physics, Govt. Post Graduate college Jampur, Pakistan.*
[c]*Department of Polymer Science and Engineering, Zhejiang University, Hangzhou 310037 PR China*

In this paper we report the synthesis, electrical and thermal properties of Polypyrrole, Polyaniline and Polyaniline-Polystyrene sulphonic acid composite. The incorporation of Polyaniline in Polystyrene sulphonic acid (PSSA) is clearly indicated by the Fourier transform infrared spectroscopy (FTIR). Differential scanning calorimeter (DSC) thermograph shows three step transitions in Polyaniline-Polystyrene sulphonic acid composites. Frequency dependent dielectric constant, dielectric loss and ac conductivity are studied in the range 1MHz to 3GHz. The ac conductivity shows a plateau like behavior in the low frequency region and it shows dispersion in the high frequency region. The variation of dielectric constant and tangent loss is the net effect of external and internal ac field. The variation of ac conductivity with frequency shows that the electrical conduction is mainly due to electron hopping.

(Received January 5, 2016; Accepted May 2, 2016)

Keywords: Fourier transform infrared spectroscopy (FTIR); Differential scanning calorimeter (DSC); Dielectric constant; Thermo gravimetric analysis (TGA).

1. Introduction

The study of conducting polymers was first introduced by shirakawa *et al*. in 1977 [1]. The chemical and physical properties of the conducting polymers which appears from their unique π-conjugation have attracted much attention of the researchers [2]. The extensively studied polymer is polypyrrole (PPy) because it is easy to synthesize, light in weight and stable in the environment [3]. In the last decades conjugated polymers have received significant interest as these are suitable to be used in electronics and its related fields. Polyaniline (PAni) is considered as one of the best material that can be used in electronics due to its processability and stability. Conducting polymers are used in advance applications like gas sensors, plastic batteries, electro chromic displays, super capacitor, electronic, drug delivery, corrosion protection, EMI shielding, nonlinear optics, gas separation membranes, humidity sensors and enzyme immobilization [1-5]. The poor mechanical properties of the conducting polymers have limited their applications but some have excellent mechanical and thermal properties. The electrical conductivity of these polymers lies between 10^{-5} S/cm and 10^{-2} S/cm while the insulators which are commonly used have conductivity below 10^{-12}S/cm [7]. One of the most promising organic conducting polymers PAni emerged due to its low cost, good environment stability, high polarization yield and moderate conductivity [8]. The unique properties of the polypyrrole (PPy) have fascinated the researchers as it is simple to synthesize, good mechanical properties and highly conductive. Polypyrrole (PPy) can be synthesized by the chemical polymerization method and is insoluble in common organic solvents due to its strong inter chain interaction. The important green chemistry is based on the preparation of multifunctional conducting polymers and their derivatives by

* Corresponding author: mrkhichi@gmail.com

oxidative polymerization [9]. The foremost work on the preparation of conducting polymer "Aniline Black" was published in 1862 [10]. It was synthesized at that time by the anodic oxidation of aniline and it changes a colour upon applying a potential that is why it is laterally known as electrochromic material at that time its electrical properties were not measured [11]. MacDiarmid reported first time that aniline is an acid aqueous solution in 1985 which can be oxidized chemically by using an oxidant ammonium peroxydisulfate (APS) to obtain green powder of PAni having good conductivity [12, 13]. In this paper we have synthesize and studied the comparative electrical and thermal behavior of PAni, PPy and PAni-PSSA composite.

2. Experimental

2.1 Materials

All the chemicals which are used in this study are of analytical grade. Aniline monomers having 99% purity are of Sigma Aldrich and polystyrene sulfonic acid (PSSA) is purchased from Alfa Aesar (wt 30% water solution, Mw75000). Pyrrole (Py) having purity 95%, ammonium persulfate (APS) are obtained from Fluka.

2.2 Preparation of sample for Measurements

In order to measure the electrical properties, the material was grinded with the help of mortar and pestle; the powder was pressed in to pellets under the load of (~60 KN) by using the Paul-Otto weber Hydraulic press. The diameter of the pellet was 6 mm while its thickness was 3 mm. The dielectric measurements were taken by the help of Agilent 4287A and the frequency range was 1 MHz to 3 GHz. TG and DSC were measured on STA 409 Cd and the heating rate was kept at 10°C/min.

2.3 Synthesis of Polyaniline

Take 5 ml aniline and put it in a 50 ml deionized water and stir it vigorously for half an hour then add 5 ml Hydrocholoric acid (HCl) and finally add 6.125 g ammonium peroxydisulfate (APS) Greenish black colour will appear then place the beaker at a very low temperature of 5°C for 24 hour so that polymerization will take place. Finally wash the material with deionized water many times so that the residual material becomes colorless.

2.4 Synthesis of Polypyrrole (PPy)

The monomers of pyrrole are polymerized by chemical oxidative polymerization method. Take 0.6 M of ferric chloride hexahydrate and dissolve it into 50 ml deionized water. Add 0.2 M of pyrrole drop wise in the 0.6 M solution of $FeCl_3.6H_2O$ under constant stirring and maintaining a temperature of 8°C for 1hour by using the liquid nitrogen. The obtained black precipitates are washed several times with deionized water followed by ethanol until the washed material becomes clear. The powder of polypyrrole is dried in an oven at 60°C for one hour.

2.5 Synthesis of water soluble PAni-PSSA

The water soluble PAni-PSSA is prepared by chemical oxidative polymerization method in which ammonium persulfate (APS) can be used as an oxidant [14, 15]. In this process 7.5 g of PSSA is added into 20 ml deionized (DI) water and put it into a flask then 0.2 ml of aniline is added and the mixture is kept on stirring for one hour. Drop 10 ml of aqueous solution of ammonium persulfate (APS) (0.05 g/ml) into the mixture. After it the mixture is stirred for half an hour, and stood for another 12 hours. Finally the resultant is precipitated then washes it with acetone and deionized water. Dry the powder under vacuum at room temperature for 48 hours to obtain a dark-green powder of Polyaniline-Polystyrene sulfonic acid.

2.6. Dielectric Evaluation

The complex dielectric permittivity can be written as $\varepsilon^*(\omega) = \varepsilon'(\omega) - j\varepsilon''(\omega)$ where ε' and ε" are the real and imaginary part of the permittivity respectively, with $j=\sqrt{-1}$. The following

parameters such as equivalent capacitance (C), dissipation factor (D) can be used to calculate the dielectric constant by the help of Agilent meter at different frequencies. The commonly employed relations are as under;

$$\varepsilon'(\omega) = c\,(\omega)\frac{d}{A} \tag{1}$$

$$\varepsilon''(\omega) = \varepsilon'(\omega)\tan\delta \tag{2}$$

$$\sigma_{ac}(\omega) = \omega\varepsilon_0\varepsilon''(\omega) = \omega\varepsilon_0\varepsilon'(\omega)\tan\delta \tag{3}$$

Where σ_{ac}, d, A, D (tanδ), δ represent ac conductivity, thickness, effective area of the sample, dissipative factor and phase angle, respectively. The electrical properties of a polymer composite cannot be described by the complex permittivity. It is essential to calculate the electric modulus M*(ω) which is very helpful for the detail study of the electrical properties of a polymer composite. The concept about electric modulus was introduced by McCrum et al [14].
The real and imaginary part of the electric modulus M*(ω) can be calculated from ε*(ω),

$$M^*(\omega) = \frac{1}{\varepsilon^*(\omega)} = M' + jM'' \tag{4}$$

Where the real part of electric modulus $M^*(\omega)$ is:

$$M'(\omega) = \frac{\varepsilon'}{\varepsilon'^2 + \varepsilon''^2} \tag{5}$$

And the imaginary part of electric modulus $M^*(\omega)$ is as under

$$M''(\omega) = \frac{\varepsilon''}{\varepsilon'^2 + \varepsilon''^2} \tag{6}$$

The complex dielectric permittivity $\varepsilon^*(\omega)$ is a factor that lies between alternating electric field $\vec{E}(\omega)$ and polarization (P) of the material [15, 16].

Polarization relation can be written as;

$$\vec{P}(\omega) = (\varepsilon^*(\omega) - 1)\varepsilon_0\,\vec{E}(\omega) \tag{7}$$

Where ε_0, ω are the permittivity of the free space and angular frequency respectively. The data for complex permittivity depends on the physical properties like pressure, temperature, frequency and composition of the used materials. In the light of statistical mechanics both ε' and ε" have important physical meaning; where ε', ε" stands for the energy stored per cycle and for the energy loss per cycle, respectively. Dielectric spectroscopic is categorized into two ways. One is the frequency domain measurement and other one is time domain. In case of frequency domain sinusoidal alternating field is applied while in case of time domain step like electric field is applied to the sample. The complex dielectric permittivity is related to the free oscillation in an ac electric field as described by Havriliak-Negami relation [17-19].

3. Results and discussions

The maximum value of dielectric constant appears at low frequency is the result of interfacial dislocation pile up, grain boundary defect and oxygen vacancies etc. Dielectric constant varies with frequency depicts the dispersion due to Maxwell Wagner interfacial polarization that is in agreement with Koop's phenomenology theory [20-23]. The data shows that the dispersion of the dielectric constant at low frequency comes from the grain boundary and at high frequency it

comes from the grains. The value of the real part of dielectric constant decreases with the increase of frequency, the variation of the real part of dielectric constant with frequency is shown in Fig. 1. Electrons are distributed around the nuclei evenly in the absence of an electric field but at the application of electric field; electron cloud is from the nuclei in the direction opposite to the applied field. As a consequence, the separation between the negative and positive charge take place and the molecule behave like an electric dipole. Three modes of polarization occur that are electronic polarization, atomic polarization and orientation polarization [24]. The loss in dielectric arises from the inability of polarization in a molecule to follow the rate of change of the oscillating applied electric field. The dielectric constant values of PAni-PSSA, PAni and PPy decreases with increasing frequencies. The decrease in dielectric constant with frequency is due to either the lag of dipole oscillations behind those of the applied ac electric field at high frequencies or due to more need of thermal energy to disturb the ordered dipoles at higher frequencies of the applied field [25]. At low frequency, the values of the real dielectric constant of PAni-PSSA show the energy stored ability in the composite is high as compared to polymer PAni and PPy and at high frequency the values of polymers are same but composite value is slight high. The dielectric material with a heterogeneous structure can be imagined as a structure consists of well conducting grains separated by highly resistive thin layers called grain boundaries. In this case, the applied voltage acts on the small particles (grains) and a space charge polarization is build up at grain boundaries. Space charge polarization is due to the conductivity of the grains and the presence of the free charges at the grain boundary. Koop's proposed that the effect of grain boundaries is predominant at low frequencies. The high value of the dielectric constant is the result of the thinner grain boundaries. The materials which have low dielectric constant are preferred for high frequency applications. The low dielectric constant materials have remarkable penetration depth ability for the electromagnetic waves and these reduce the skin effect [26-30].

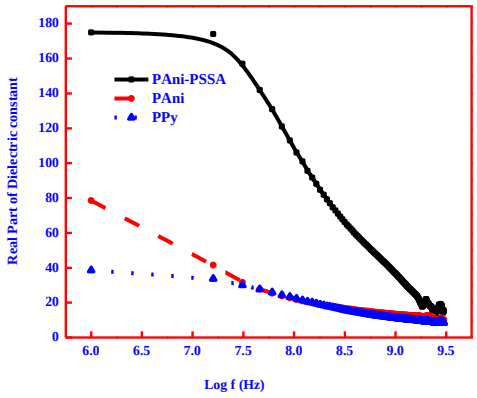

Fig. 1. Graph b/w real part of Dielectric constant and log f (Hz).

The imaginary part of the dielectric constant versus frequency is shown in Fig. 2. The decrease in the imaginary part of dielectric constant with increase in frequency agrees well with the Debye relaxation process. The maximum value in the imaginary part is observed when the hopping frequency is equal to the external electric field frequency. The value of imaginary part of dielectric constant attains a maximum value then it decreases due to the power loss [31]. The dissipation of energy is more in the composite as compared to polymer PAni and PPy.

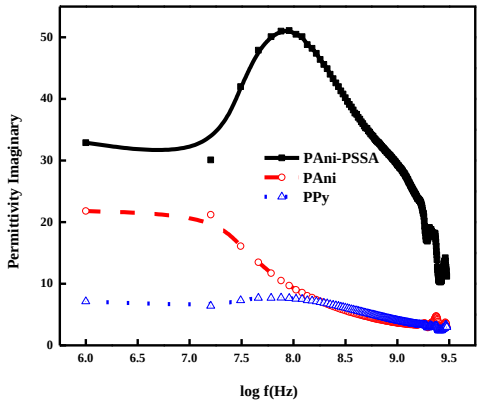

Fig. 2. Graph b/w Imaginary part of Dielectric constant and log f(Hz).

Fig. 3 shows the Tan loss has a high value in case of PAni-PSSA as compared to Polymers PAni and PPy. The dielectric analysis data for polymeric materials and its composite have a great importance when it is measured in a particular frequency range. Its precise knowledge is essential to investigate the dielectric feature and related properties. The higher dielectric loss is observed for PAni-PSSA which might be due to increase in interaction that leads to higher crystallinity.

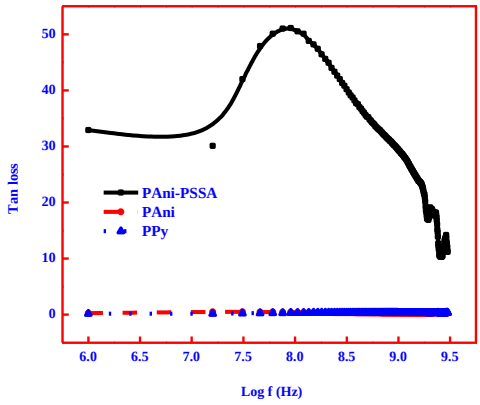

Fig. 3. Graph b/w Tan loss and log f(Hz)

The electric modulus is just the reciprocal of complex dielectric permittivity.

$$M^*(\omega) = \frac{1}{\varepsilon^*} \tag{8}$$

Fig.4 and Fig.5 show the frequency dependence of real part of electric modulus (M') and imaginary part of electric modulus (M″) of PAni, PPy, PAni-PSSA. At high frequency, the real part of electric modulus M' shows dispersion while at low frequency it tends to zero which shows the low contribution of electrode polarization to M'. At high frequency dielectric relaxation peaks take place when the hopping frequency of the localized electric charge carriers becomes approximately equal to that of the externally applied ac electric field.

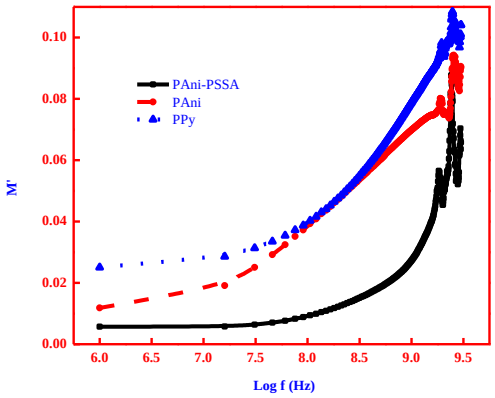

Fig. 4. Graph b/w real part of Electric Modulus and log f(Hz)

It is obvious from the figure that at lower frequencies the imaginary part of electric modulus M″ exhibit low value which may be due to the large value of capacitance associated with the electrode polarization and at high frequency it shows high values as a consequence of low value of capacitance [32].

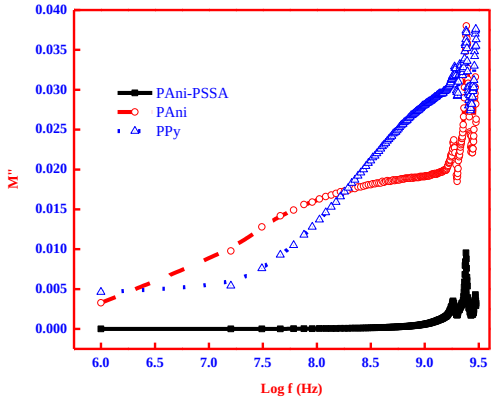

Fig. 5. Graph b/w Imaginary part of Electric Modulus and log f(Hz)

The ac conductivity of PAni, PPy, and PAni-PSSA composite were studied and it was found to be a function of frequency as shown in Fig. 6. The frequency dependent ac conductivity showed a plateau in the low frequency region and dispersion at high frequency region. In the low frequency region the conductivity is independent of frequency and at high frequency, it is frequency dependent. The early trend in the low frequency region is due to the free charges available in the polymer matrix and the later one is due to the trapped charges which are only active at high frequency [33-35]. In case of PAni-PSSA the presence of substituents attached with the main chain of PAni may be the cause of decrease in the electrical conductivity [36]. The variation of the ac conductivity with the frequency at room temperature σ_{ac} shows a normal behavior, it increases with the increase of frequency. Frequency dependence of ac conductivity $\sigma(\omega)$ follows the relation [37].

$$\sigma(\omega) = A\omega^{n} \tag{9}$$

Where $\omega = 2\pi f$, n is dimensionless exponent and A has the dimensions of $\Omega^{-1}cm^{-1}$ Dielectric constant and ac conduction mechanism are strongly correlated as it is noted by Zhang et al [38].

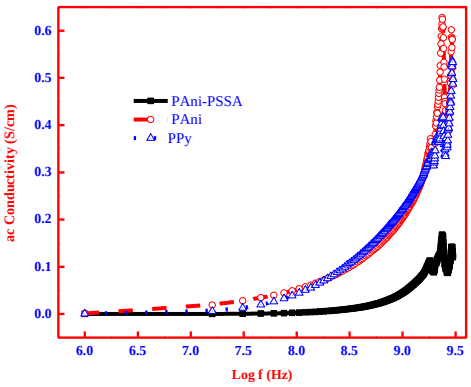

Fig. 6. Graph b/w ac Conductivity and log f(Hz)

The quality factor (Q = $\frac{1}{tan\delta}$) is shown in Fig. 7. The maximum value of the quality factor of PAni, PPy and PAni-PSSA indicate that these materials can be used in various industrial applications; as these have minimum loss values. The obtained values of quality factor are comparatively high as compared to the rare earth doped soft ferrites [39].

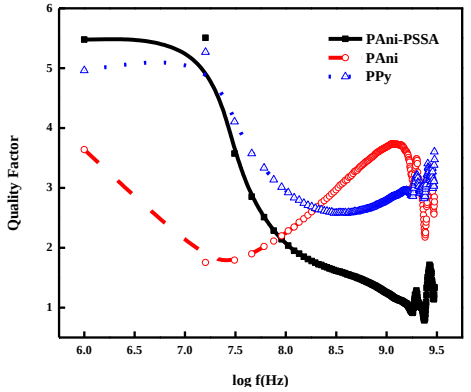

Fig. 7. Graph b/w Quality factor and log f(Hz)

The variation of resistivity with frequency is shown in Fig.8. At low frequency the resistivity is high its mean, the grain boundary plays an important role but as the frequency becomes high, the resistivity becomes low; so the grains play an effective role at the high frequency and resistivity decreases with the increase of frequency.

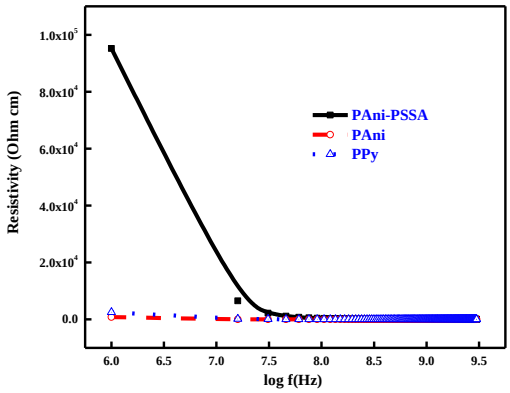

Fig. 8. Graph b/w Resistivity and log f(Hz).

Impedance values are measured at the room temperature. The high values of the impedance show the limited adsorption of water molecules. It is clear from the Fig. 9 that in Polypyrrole the adsorption of water molecule is more limited as compare to PAni, PAni-PSSA composite. The values of the main parameters like real dielectric constant, Imaginary dielectric constant, tangent loss, ac conductivity and capacitance are given in the table I. The value of the tangent loss is small in the polymers PAni, PPy as compared to composite PAni-PSSA.

Table. I The values of different parameters at a high frequency log f = 9.5Hz

Name	ε'	ε''	tan δ	σ_{ac} (S/cm)	C (PF)
PAni-PSSA	16	13	12	0.1	4.5
PAni	12	05	0.8	0.6	0.45
PPy	09	03	0.8	0.5	0.38

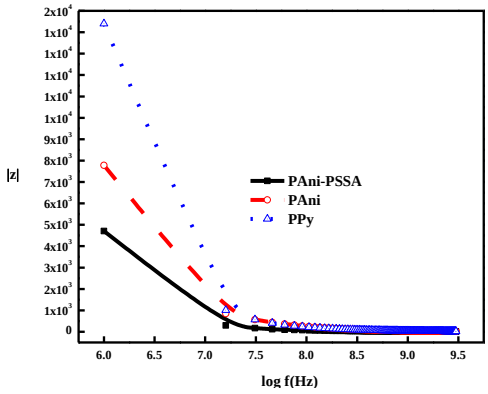

Fig. 9. Graph b/w Impedance and log f(Hz)

The capacitance value is high at low frequencies but it is low at high frequencies as shown in Fig.10. In fact, the alternating voltage half period becomes shorter at high frequencies so the space charge polarization fails to settle itself and capacitance begins to drop. The time required for electronic or ionic polarization to set in is very small as compared with the time of voltage sign change between the two half-period of the applied alternating voltage. The variation of capacitance with frequency is given by the relation [40].

$$C = C_g + [s\tau/(\omega^2\tau^2 + 1)] \quad (10)$$

Where C_g is geometrical capacitance, s is conductance corresponding to absorption current, τ is the dipole relaxation time and ω is the angular frequency. According to this, capacitance is maximum when ω = 0 and minimum when ω = ∞ [40].

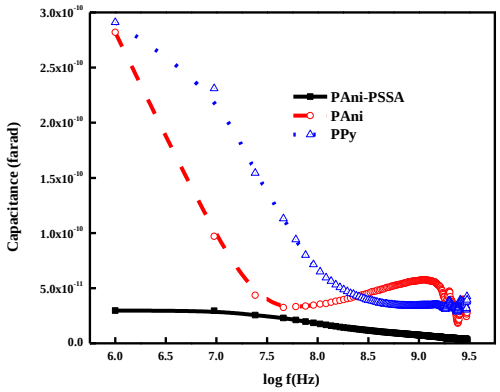

Fig. 10. Graph b/w Capacitance and log f(Hz)

Thermogravimetric analysis (TGA) and the derivative of weight loss (DTG) for PAni-PSSA are shown in Fig. 11. It is clear from the DTG curve of PAni-PSSA three significant events takes place. The initial event show the decomposition due to water or moisture evaporation up to 140°C, a second event is the decomposition in the range 140°C to 250°C, it is due to oligomer and in the last event major weight loss after 425°C is due to the decomposition of polymer. The same behavior is reported in the literature by Gupta Neetika et al [41].

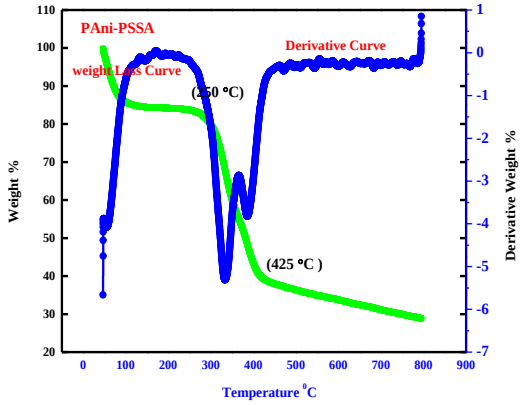

Fig. 11. TGA/DSC curve of PAni-PSSA.

The TGA curve and the derivative of weight loss (DTG) curve of PAni show that there are three main stages of weight loss, the first one below 100°C being due to the release of free water. The second stage with a maximum weight loss rate at 200°C is due to the loss of chemically combined dopant (HCl). In the third stage PAni itself decomposes, the range of temperature is 500°C to 700°C [42].

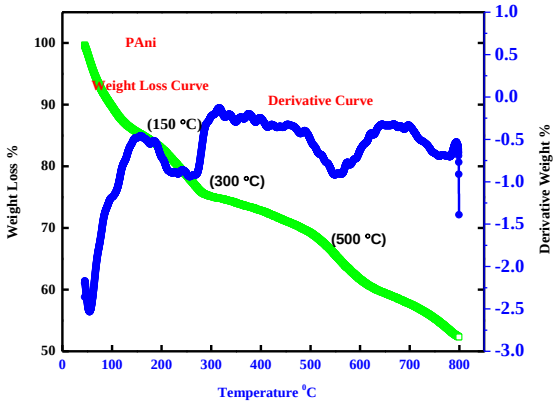

Fig. 12. TGA/DSC curve of PAni.

The TGA curve of PPy exhibited two stages weight loss, the first stage starts from 180°C and the percentage loss is 5%, second degradation starts at 350°C and the percentage loss is 15% as it is reported by many researchers [43, 44]. We also observe the same behavior so the curve is not depicted here. The characteristics absorption bands of PAni are at 1473 C-N (stretching of the quinoid ring), 1308 (C-N stretching), 1114cm^{-1} a vibration mode of N=Q=N (Q represents quinoid ring). The band at 1308cm^{-1} is related to the stretching vibration of charged nitrogen segment and provides information about the delocalization in the PAni chains. The characteristics peaks of PAni appear at 1473cm^{-1} and 1567cm^{-1}, these bands are ascribed to the stretching vibration of benzonoid and quinoid rings respectively. The characteristics peak at 1567cm^{-1}, 1503cm^{-1}

corresponds to the C=C stretching of quinoid and benzonoid rings respectively. The band at 3432cm^{-1} is relating to O-H stretching mode, 2930 cm^{-1} is assigned to the C-H stretching mode. The band at 790cm^{-1} is related to the C-S stretching vibration. The absorption at 2356 cm^{-1} emerges which corresponds to N-H stretching mode of primary amine cation in aniline salts. The bands at 1114cm^{-1} and 790cm^{-1} are distinctive features of C-H in plane and C-H out of Plane bending [45].

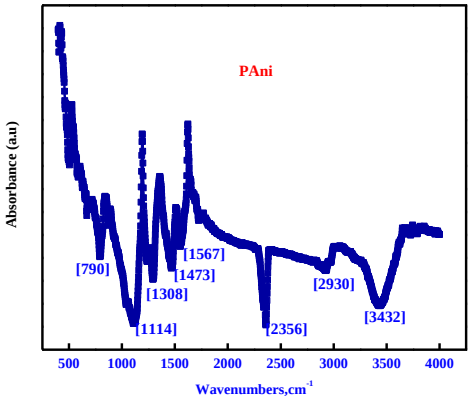

Fig. 13. FTIR spectroscopic curve of PAni.

In the spectrum of PAni-PSSA the peaks at 1608cm^{-1} and 1406cm^{-1} corresponds to the C=C stretching deformation of quinoid and benzonoid rings, respectively. The peak at 1130 cm^{-1} is due to C-N stretching of secondary amine while the absorption at 842cm^{-1} is assigned to the out of plane deformation of C-H in the 1,4-disubstituted benzene ring. Moreover, the peak at 1009 cm^{-1} ascribed to $-SO_3^-$ group was also observed in the spectrum of the soluble PAni-PSSA. All these show that PAni has been successfully obtained and PSSA has been incorporated into the soluble product [45].

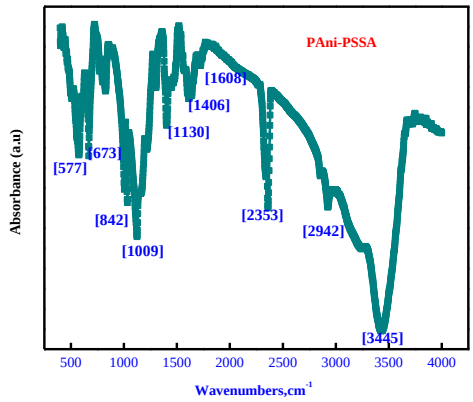

Fig. 14. FTIR spectroscopic curve of PAni-PSSA.

The peak at approximately 3165cm^{-1} is attributed to the hydrogen bonded N-H stretching vibration. Fig. 15 shows the FTIR spectrum of polypyrrole, the band at 1557cm^{-1} and weak band at 1468cm^{-1} are assigned to the stretching vibration of C=C and C-C in the pyrrole ring [40,41]. The peak at approximately 1652cm^{-1} and approximately 1547cm^{-1} could be attributed to C-N and C-C asymmetric and symmetric ring stretching respectively. Additionally the peak near approximately 1191cm^{-1}, 1088 cm^{-1} represents the doping state of PPy and the peak at 618 cm^{-1} is due to Fe^{+2} [46].

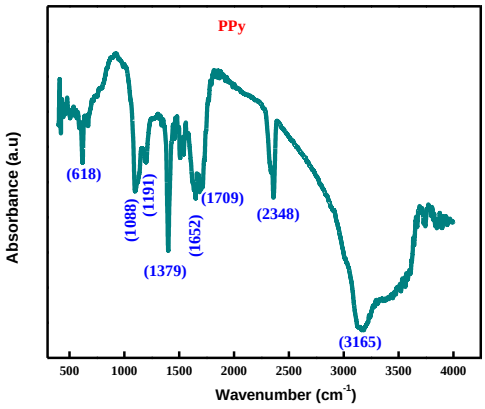

Fig. 15. FTIR spectroscopic curve of PPy

4. Conclusions

FTIR spectra of synthesized composite PAni-PSSA confirm the existence of conductive polyaniline. The ac conductivity showed a plateau in the low frequency region and dispersion at the high frequency region. The increase in ac conductivity was due to the creation of additional hopping sites in the polymeric composite. Thus the frequency dependent ac conductivity could be attributed to the hopping mechanism. The dispersion of ac conductivity is explained on the basis of Maxwell-Weigner and Koops model. PPy and PAni have a low dielectric constant values so these can be used for EMI shielding and in high frequency application purpose. The high value of dielectric constant of PAni-PSSA is due to its thinner walls of the grain boundaries. The adsorption of water is more limited in PPy as compare to PAni and PAni-PSSA. PAni and PPy have a high dielectric constant and low dielectric loss so these can be used in high speed computers.

Acknowledgement

Corresponding author (Ghulam Murtaza) is thankful to Higher Education Commission (HEC) of Pakistan for providing financial assistance through IRSIP scholarship.

References

[1] H. Shirakawa, E. J Louis, A. G, Mac Diarmid, C. K Chiang, A. J Heeger, J. Chem. Soc. Chem. commun, **16**, 578 (1977).
[2] J. Jang, Y. Nam, H. Yoon, Adv. Mater. **17**, 1382 (2005).
[3] Wu T. –M, Lin S. –H, J. Pol. Sc. A **44**, 6449 (2006).
[4] N. Gupta, D. Kumar, S. K. Tomar, Int. J. of Mater. and Chem., **2**(2), 79 (2012).
[5] C. S. Stan, M. Popa, M. Olariu, M. S. Secula, Open Chem, **13**, 467 (2015).
[6] B. Kim, V. Koncar, E. Devaux, AUTEX Research Journal, **4**(1), 9 (2004).
[7] C. –P. Chwang, C. –D. Liu, S. –W. Huang, D. –Y. Chao, S. –N. Lee, Syn. Met. **142**, 275 (2004).
[8] A. Imani, G. Farzi, A. Ltaief, Facile Int. Nano Lett. **3** (52), (2013).
[9] H. Letheby, J. Chem. Soc., **224**, 161 (1862).
[10] M. E. Goppelsroder. Compt. Rend., **82**, 331 (1876).
[11] J. C. Chiang, A. G. MacDiarmid, Synth.Met **13**, 193 (1986).
[12] C. Lucignano, F. Quadrini, L. Santo, J. of Comp. Materials, **42**, 2841 (2008).
[13] L. H. Abound, Natural and Applied Sciences. **4**, 73 (2013).

[14] N. G, McCrum B E, Read Williams G. Wiley, (London) (1967).
[15] M. A. El-Shahawy, A. F. Mansour, H. A. Hashem, J. Pure Appl. Phys **36**, 78 (1998).
[16] C. J. F. Böttcher, P. Bordewijk, *Theory of dielectric polarization*, Elsevier (Amsterdam), (1973).
[17] M. Cook, D. C. Watts, G. Williams, Trans *Faraday Soc*. **66**, 2503 (1970),
[18] N. E. Hill, W. E. Vaughan, A. H. Price, M. Davis, Dielectric Properties and Molecular Behaviour, Van Nostrand(London), (1969).
[19] C. F, Böttcher, P Scaife, *Principles of Dielectrics* Oxford University Press (Oxford), (1989).
[20] K. S. Lee, G. B. Blanchet, F. Gao, Y. L. Loo, Appl. Phys. Lett. **86**, 074102 (2005),.
[21] J. C. Maxwell, A. Treatise on electricity and Magnetism,. Oxford, NewYork 2, (1954).
[22] K. W. Wagner, Ann. Phys. **40**, 817 (1913).
[23] C. G. Koops, Phys. Rev. **83**, 121 (1951),.
[24] S. Kazan, E. E. Tanriverdi, R. Topkaya, S. Demirci, O. Akman, A. Baykal, B. Aktas, J. of Chem. (2012).
[25] S. V. Jadhav, V. Puri, Synth. Met. **158**, 883 (2008).
[26] S. M. Reda, Dyes Pigments **75**, 526 (2007).
[27] F. Latif, M. Aziz, N. Katun, M. Ali, M. Z. A. Yahya, *J. Power Sources*. **1594**, 1401 (2006).
[28] S. Havriliak, S. Negami *J. Polym. Sci. Part-C.* **14**, 99 (1966).
[29] J. C. Maxwell, Electricity and Magnetism, Oxford University Press, London, 1, (1873).
[30] B. A. Afzal, M. J. Akhtar, M. Nadeem, M. M. Hassan, J. Phys. Chem C, **113**, 17560 (2009).
[31] B. Zhou, Y. W. Zhang, C. S. Liao, F. X. Cheng, C. H. Yan, J. of Mag. and Mag.Materials **247**, 70 (2002).
[32] S. Fang, C. H. Ye T. Xie, Z. Y. Wong, J. W. Zhao, L. D. Zhang, *Appl. Phys. Lett*. **88**, 013101 (2006),.
[33] S. B. Aziz, Z. H. Z. Abidin, A. K. Arof, eXPRESS Polymer Letter, **4**(5), 300 (2010).
[34] H P, de Oliveira, M. V. B. dos Santos, C.G. dos Santos, C. P. de Melo, *Mater. Charact.* **50,** 223 **(**2003),.
[35] H. P. de Oliveira, M. V. B. dos Santos, C. G. dos Santos, C. P. de Melo, *Synth. Met*. **135,** 447 (2003),.
[36] P. B. Macedo, C. T. Moynihan, R. Bose, *Phys. Chem. Glasses.* **13,** 171 (1972).
[37] M. T. Ramesan, Polymer Plastic Technology and Engineering, **51**, 1223 (2012).
[38] Z. Kezhao, Fredkin, R. Donald, J Appl. Phys, **85**, 6187 (1999).
[39] E. Ateia, M. A. Ahmed, A. K. El-Aziz, J. Magn.Mag. Mater.**311**, 545 (2007).
[40] G. Murtaza, I. Ahmad, J. Wu, Mater. Sc. in Semicond. Process. **34**, 269 (2015).
[41] N. Gupta, D. Kumar, S. K. Tomar, Int. J. of Materials and Chem**, 2**(2), 79 (2012).
[42] Q. M. Jia, S. Y. Shan, Y. M. Wang, Poly. Mater. Sc. and Engg. **9**, 159 (2010).
[43] Y. Li, B. Ying, L. Hong, M. Yang, Syn. Met.160, **455** (2010).
[44] M. Selvarange, S. Palraj, K. Murathan, G. Rajgopal, G. Venkatachari, J. Synth. Met, **158**, 3499 (2004).
[45] M. T. Ramesan, J. Applied Polymer Sc., (2013), 1540-1546.
[46] V. T. Bhugul, G. N. Choudhari, **5**(1), 1 (2015).
[47] N. Su, H. B. Li, S. J. Yuan, S. P. Yi, E. Q. Yin, eXPRESS Polymer Letters, **6**(9), 697 (2012).